We are IntechOpen,
the world's leading publisher of
Open Access books
Built by scientists, for scientists

6,900
Open access books available

186,000
International authors and editors

200M
Downloads

154
Countries delivered to

Our authors are among the

TOP 1%
most cited scientists

12.2%
Contributors from top 500 universities

CLARIVATE ANALYTICS

**BOOK
CITATION
INDEX**

INDEXED

WEB OF SCIENCE™

Selection of our books indexed in the Book Citation Index
in Web of Science™ Core Collection (BKCI)

Interested in publishing with us?
Contact book.department@intechopen.com

Numerical Simulation of Fabrication for Ceramic Tool Materials

Bin Fang*, Chonghai Xu, Fang Yang, Jingjie Zhang and Mingdong Yi
School of Mechanical and Automotive Engineering, Shandong Polytechnic University,
P. R. China

1. Introduction

Ceramic materials have good mechanical properties, such as high hardness, good wear resistance and elevated-temperature anti-oxidation. So, Ceramic materials are widely applied not only in the field of aeronautics and astronautics, building and mechanics in modern technology, but also in the field of the cutting tool materials. Ceramic tool materials are widely used in the dry cutting and high speed cutting. The preparation of ceramic tool materials includes powdering, forming, hot-press fabrication and machining process. A green compact before sintering is a porous packing of loose powder that is held together by weak surface bonds. The individual particles fabricated together to form a dense, strong monolithic part by sintering. The driving force for the sintering is the reduction in surface free energy of the particle. This reduction is performed by diffusion transport of material. Many factors affected the process of material transport and the exhalation of pores. Therefore, the hot-press fabrication is a very complicated process in which the compact formed of fine powder materials fabricated at the temperature below the melting point of the main constituent for the purpose of gaining the enough strength of the compact by bonding particles together. The hot-press fabrication is a key process, which governs the mechanical properties of the ceramic tool materials as well as the components and content.

Most sintering theory models are based on the simple assumption of particle shape and the mass-transport mechanisms. With the rapid development of the computer simulation technology and the computational material science, modeling and numerical simulation of ceramic sintering process becomes a new and promising approach to investigate the sintering process on the micro- and meso- scale or macro-scale (Jagota& Dawson, 1990; Bordère, 2002; Wakai et al, 2004, 2005; Mori, 2006; German, 1998). At the same time, it is very significant to simulate Microstructural evolution of sintering process on the micro- and meso-scale for the theory development and the evaluation of relationship between the mechanical properties and the microstructure of ceramic materials (Guo, 1998). The two-dimensional Monte Carlo grain-growth simulation methods, firstly developed by Srolovitz and co-workers (Anderson et al, 1984; Srolovitz et al, 1984), is lately extended into the three dimensional simulation. Monte Carlo Potts' model is largely applied to simulate the solid-phase sintering process of ceramics (Hassold et al, 1990; Chen et al, 1990; Tikare & Holm,

---

* Corresponding Author

1998; Tikare et al, 2003) . Because of no assumption of the particle shape, the model can be properly used to simulate the mass-transport mechanisms. Computer simulation of final-stage sintering process of ceramics is initially developed by Hassold G N with Monte Carlo Potts' model (Hassold et al, 1990; Chen et al, 1990; Tikare & Holm, 1998). Tikare V et al (Tikare et al, 2003) simulated the densification of ceramic sintering processes with Monte Carlo Potts' model, which is coupled with vacancy-annihilation method. However, the mentioned simulation methods are only applied to simulate the sintering processes for one-composition, single-phase ceramic system. To meet the need of the severe cutting conditions and the durable tool-life in high speed cutting process, ceramic tool materials should have good mechanical properties, such as high hardness, high flexural strength, high fracture toughness, good wear resistance and elevated-temperature anti-oxidation. In order to improve the mechanical properties further, the second-phase powders are combined on the base of matrix powder to develop the composite ceramic tool materials by hot-press fabrication (Lang, 1982; Guo, 1998, Mukhopadhyay et al, 2007; Belmonte et al, 2006).

In this paper, the new Monte Carlo Potts' model for simulating the sintering process of single- and two-phase ceramic materials is developed and the two-dimensional (2D) grain-growth process is successfully simulated with considering the presence of pores in the green compact. A detailed description of the new Monte Carlo Potts model and simulation procedure is presented. The simulation results are also discussed.

2. Porosity and mean pore size of green compact

2.1 Porosity of green compact

Although the fine powders of ceramic are tightly packed by the effect of the pre-pressure and the gravity, the pore is present among the powders. Assuming the fine powders are the sphere which is equal in the radius, the porosity can be calculated by the ball-packed model.

According to the crystal structure of metallurgy (Jin et al, 2002) , as Fig.1 was shown, it is a hypothesis that there are three types of the particle arrangement, the body-centered cubic (BCC), the faceted-centered cubic (FCC) and the hexagonal closed-packed (HCP).

The porosity of three types of the particle arrangement is given by Eq. (1), Eq. (2) and Eq. (3), respectively.

1.   Porosity of BCC

$$f_{\text{BCC}} = 1 - \frac{2 \times \frac{4}{3}\pi R^3}{\left(\frac{4}{\sqrt{3}}R\right)^3} = \frac{\sqrt{3}}{8}\pi \approx 0.32 \tag{1}$$

2.   Porosity of FCC

$$f_{\text{FCC}} = 1 - \frac{4 \times \frac{4}{3}\pi R^3}{\left(\frac{4}{\sqrt{2}}R\right)^3} = \frac{\sqrt{2}}{6}\pi \approx 0.26 \tag{2}$$

3.   Porosity of HCP

$$f_{\mathrm{HCP}} = 1 - \frac{2 \times \dfrac{4}{3}\pi R^{3}}{6 \times \dfrac{\sqrt{3}}{4} \times \sqrt{\dfrac{8}{3}} \times (2R)^{3}} = \frac{\sqrt{2}}{6}\pi \approx 0.26 \qquad (3)$$

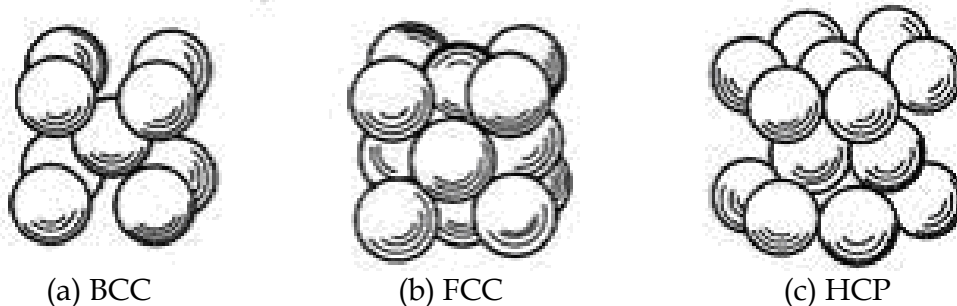(a) BCC   (b) FCC   (c) HCP

Fig. 1. Schematic Diagram of Three Type of the Particle Arrangement (Jin et al, 2002)

The particle arrangement of green compact is not as tight as the atoms in the crystal structure of metallurgy. The particle size has some distribution, and the smaller particles in the size are filled into the bigger hole. So, it is proper that the porosity of green compact is 30% during the simulation.

2.2 Mean pore size of green compact

Pore size is a function of the particle size, the particle shape and the density of the green compact in the green compact. For the specific particle size and density, the mean pore size of green compact is given by Eq. (4) (Myers et al, 1989).

$$d = \frac{2D(1-f)}{3f} \qquad (4)$$

where, d is mean pore diameter, D is powder particle diameter and f is the density of green compact.

As mentioned above, the porosity is 30% in the initial simulation system, that is to say, the value of f is 0.7. According to Eq. (4), the mean pore diameter (d) is 0.29D. Therefore, during the initialization of simulation system, the function of pore initialization is implemented when the particle diameter is the finial initialized particle size. Then, the initialized process is not finished until the required particle size is obtained.

3. Simulation method

The two-dimension Monte Carlo Potts simulation model utilizes two different approaches to simulate the grain growth and annihilation of pore (Braginsky et al, 2005) . It can model the following processes:

1.   Simulation of grain growth by short range diffusion of atoms from one side of grain boundary to the other side;

2. Simulation of long range diffusion of pores by the surface diffusion and of vacancies/material by grain boundary diffusion;
3. Simulation of vacancy-annihilation at grain boundaries.

3.1 Monte Carlo Potts model of single-phase ceramic tool materials containing pores

In the Monte Carlo Potts' model for simulating the sintering process of single-phase ceramic tool materials with pores, the fine powders and pores are mapped onto a set of two-dimensional and discrete hexagonal sites. In order to describe the state of a site i, two parameters, S_i and P_i, are required. S_i represents the orientation of the grain that the site belongs to. P_i represents the phase state of the site. The fine powder sites are given one of Q distinct, degenerate states, where the individual state is designated by the symbol S_i. The value of S_i for the solid phase is from 1 to Q and Q is the maximum value for the grain orientation. At the same time, the P_i of fine powder sites is given 1, which is the symbol of solid. The pore sites can be assumed only one state, $S_{pore}=Q+1$, and the P_i of pore sites is given 3, which is the symbol of pore. Continuous fine powder sites of the same state S_i forms the fine powders and the value of P_i for the continuous fine powder sites are 1. Continuous pore sites forms a pore and the value of P_i for the pore sites are 3. During evolution of simulation, grain boundaries exist between neighboring grain sites of different states, S_i, and pore-grain interfaces exist between neighboring pore and grain sites. There are two different boundaries in the simulation system. The boundary-one is formed between neighboring grain sites of different states, and its energy is J_1. The boundary-two is formed between neighboring pore and grain sites, and its energy is J_2.

The equation of state for these simulations is the sum of all the neighbor interaction energies of single-phase ceramic tool materials with pores can be written as:

$$E_{Tol} = E_1 + E_2 \tag{5}$$

$$E_1 = J_1 \sum_{i=1}^{N} \sum_{j=0}^{n_1} \left[1 - \delta(S_i, S_j) \right] \tag{6}$$

$$E_2 = J_2 \sum_{i=1}^{N} \sum_{j=0}^{n_2} \left[1 - \delta(S_i, S_j) \right] \tag{7}$$

where, E_{Tol} is the total energy (J). E_1 is the energy of the neighboring grain sites (J). E_2 is the energy of the neighboring pore and grain sites (J). N is the sites number of solid phase. n_1 is the solid-phase site number around one specific site of solid phase(≤ 6). n_2 is the pore-phase site number around one specific site of solid phase(≤ 6). And $\delta(q_i, q_j)$ is the Kronecker function defined as $\delta(S_i, S_j) =1$ for $S_i = S_j$ and otherwise $\delta(S_i, S_j) =0$, with S_i and S_j denoting the orientation parameters of the neighboring sites i and j.

3.2 Monte Carlo Potts model of two-phase ceramic tool materials containing pores

In the Monte Carlo Potts' model for simulating the sintering process of two-phase ceramic tool materials with pores, the fine powders and pores are mapped onto a set of two-

dimensional and discrete hexagonal sites. In order to describe the state of a site i, two parameters, S_i and P_i, are required. S_i represents the orientation of the grain that the site belongs to. P_i represents the phase state of the site. The fine powder sites are given one of Q distinct, degenerate states, where the individual state is designated by the symbol S_i. The value of S_i for the solid phase is from 1 to Q and Q is the maximum value for the grain orientation. At the same time, the P_i of fine powder sites is assigned the value of 1 or 2, which is the symbol of solid phase-one or phase-two. The pore sites can assume only one state, $S_{pore}=Q+1$, and the P_i of pore sites is assigned the value of 3, which is the symbol of solid. Continuous fine powder sites of the same state S_i forms the fine powders and the value of P_i for the continuous fine powder sites is 1 or 2. Continuous pore sites forms a pore and the value of P_i for the pore sites is 3. During evolution of simulation, grain boundaries exist between neighboring grain sites of different states, S_i, and pore-grain interfaces exist between neighboring pore and grain sites. If two adjacent sites are phase-one and phase-two and their grain orientation is the same, then the composite grains are formed and the two phases exist diffusion each other. If two adjacent sites are single phase and their grain orientation is the same, then the grains for single phase are formed. Grain boundaries exist between neighboring grain sites of different states, S_i, and pore-grain interfaces exist between neighboring pore and grain sites. There are five different boundaries in the simulation system. The boundary-one is formed between the phase-one sites with different orientations, the boundary-two is formed between the phase-two sites with different orientations, the boundary-three is formed between the phase-one and phase-two sites, the boundary-four is formed between the phase-one and pore sites and the boundary-five is formed between the phase-two and pore sites. And their grain boundary energy is J_{11}, J_{22}, J_{12}, J_{13} and J_{23}, respectively. It is assumed that the grain boundary energy is dependent on the grain boundary and independent of the misorientation of the adjacent grains and of the grain orientation. Each of mass diffusion was performed by one site in the simulation.

The equation of state for these simulations is the sum of all the neighbor interaction energies of two-phase ceramic tool materials with pores can be written as:

$$E_{Tol} = E_{11} + E_{12} + E_{22} + E_{13} + E_{23} \tag{8}$$

$$E_{11} = J_{11} \sum_{i=1}^{N_1} \sum_{j=0}^{n_1} \left[1 - \delta(S_i, S_j) \right] \tag{9}$$

$$E_{22} = J_{22} \sum_{i=1}^{N_2} \sum_{j=0}^{n_2} \left[1 - \delta(S_i, S_j) \right] \tag{10}$$

$$E_{12} = J_{12} \sum_{i=1}^{N_3} \sum_{j=0}^{n_3} \left[1 - \delta(S_i, S_j) \right] \tag{11}$$

$$E_{13} = J_{13} \sum_{i=1}^{N_1} \sum_{j=0}^{n_4} \left[1 - \delta(S_i, S_j) \right] \tag{12}$$

$$E_{23} = J_{23} \sum_{i=1}^{N_2} \sum_{j=0}^{n_5} \left[1 - \delta(S_i, S_j) \right] \tag{13}$$

where, E_{Tol} is the total energy (J). E_{11} is the energy of the neighboring phase-one grain sites (J). E_{22} is the energy of the neighboring phase-two grain sites (J). E_{12} is the energy of the neighboring phase-one and -two grain sites (J). E_{13} is the energy of the neighboring pore and phase-one grain sites (J). E_{23} is the energy of the neighboring pore and phase-two grain sites (J). N_1 is the sites number of phase-one. N_2 is the sites number of phase-two. N_3 is the smaller sites number of that of phase-one or phase-two. n_1 is the phase-one site number around one specific site of phase-one(≤ 6). n_2 is the phase-two site number around one specific site of phase-two(≤ 6). n_3 is the phase-two site number around one specific site of phase-one when N_3 is the phase-one site number(≤ 6), otherwise, n_3 is the phase-one site number around one specific site of phase-two when N_3 is the phase-two site number(≤ 6). n_4 is the pore-phase site number around one specific site of phase-one(≤ 6). n_5 is the pore-phase site number around one specific site of phase-two(≤ 6). And $\delta(S_i, S_j)$ is the Kronecker function defined as $\delta(S_i, S_j) = 1$ for $S_i = S_j$ and otherwise $\delta(S_i, S_j) = 0$, with S_i and S_j denoting the orientation parameters of the neighboring sites i and j.

3.3 Monte Carlo algorithm

3.3.1 Simulation algorithm of grain growth

The Monte Carlo simulation of the grain growth processes is implemented by the following steps:

1. The system energy is computed using Eq. (5) for the single phase material system or Eq. (8) for the two phase material system.
2. A site is randomly selected. If the site is solid-phase and located on the boundary, a new possible crystallographic orientation of the site is randomly chosen from one set of crystallographic orientations of neighboring solid-phase site.
3. The total energy of the simulated system with a new crystallographic orientation is computed using Eq. (5) for the single phase system or Eq. (8) for the two phase system and the difference (ΔE) between the new energy and the old is calculated.
4. As shown in Eq. (14), the energy difference (ΔE) is applied to compute the transition probability for the site with a new crystallographic orientation.

$$P(\Delta E) = \begin{cases} 1 & \Delta E \leq 0 \\ \exp^{-\frac{\Delta E}{k_B T}} & \Delta E > 0 \end{cases} \tag{14}$$

where, T is the temperature of the site which is considered and k_B is the Boltzmann's constant.

5. As the transition probability $P(\Delta E)$ is calculated, a random probability R is generated in a range of 0~1. The site with a new crystallographic orientation is accepted to change into the new crystallographic orientation if R≤$P(\Delta E)$, otherwise the old site orientation is kept.
6. The system energy for the current configuration is assigned to the step (1). The simulation procedure is repeated from the step (2). The attempted N (total sites number in the simulation system) times is regarded as one Monte Carlo Step (MCS).

During the simulation, the site leaps to the nearest-neighbor cell across the grain boundary if one which belongs to the cell has attempted a crystallographic orientation of that and been accepted during the reorientation attempt, which leads to the grain-boundary migration and the microstructural evolution. The leap of the site simulates the evaporation-deposition mechanism by the atoms during the sintering processes. The cell that loses the sites starts to shrink, on the other hand, the cell that gains the sites starts to grow. So, the growth or shrinkage of grains can be properly simulated during the fabrication of ceramic tool materials in the simulation system.

3.3.2 Simulation algorithm of pore migration

In order to keep the same total number of pore sites and grain sites throughout the simulation in the simulation system, pore migration is simulated using conserved dynamics (Hassold et al, 1990).

The Monte Carlo simulation of pore migration processes is implemented by the following steps:

1. The pore site neighboring grain boundary and the solid-phase site neighboring the pore site are chosen at random.
2. The two sites are temporarily exchanged with the solid-phase site assuming a new state S where S results in the minimum energy. This minimum-energy, pore-grain exchange simulates pore migration by surface diffusion.
3. The change in energy (ΔE) for this exchange is calculated using Eq. (5) for the single phase system or Eq. (8) for the two phase system.
4. The change in energy (ΔE) is applied to compute the transition probability for the pore migration attempt with the above mentioned Eq.(14).
5. As the transition probability $P(\Delta E)$ is calculated, a random probability R is generated in a range of 0~1. The temporarily exchange is accepted if $R \leq P(\Delta E)$, otherwise the old microstructure is kept. The attempted N (total sites number in the simulation system) times is regarded as one Monte Carlo Step (MCS).

At lower temperatures, the pores do not have sufficient energy to diffuse in the grain structure, and only can coalesce into small isolated pores and stagnate microstructural evolution. Therefore, the simulation temperature of the pore migration is $k_BT=0.7$. This higher temperature is necessary for accurate simulation of pore migration (Tikare & Holm, 1998).

3.3.3 Simulation algorithm of vacancy annihilation

During Monte Carlo simulation of ceramic tool material system with pores, vacancy is defined as a single pore site which is surrounded by grain sites. The densification of material in simulation is achieved by vacancy annihilation (Braginsky et al, 2005). In DeHoff's stereological theory of sintering densification (DeHoff et al, 1989), the densification mechanism comprises vacancy migration from pores to grain boundaries and vacancy annihilation at the grain boundaries. The densification is the process of vacancies being painted on the grain boundary, with an entire monolayer of vacancies annihilated, so that the mass centers of adjacent grains move towards the grain boundary. The rate of densification is governed by the time of vacancies that diffuse and cover the entire grain

boundary. The densification is simulated with the algorithm of vacancy annihilation as shown in Fig.2. The schematic diagram of this algorithm is shown in Fig.3.
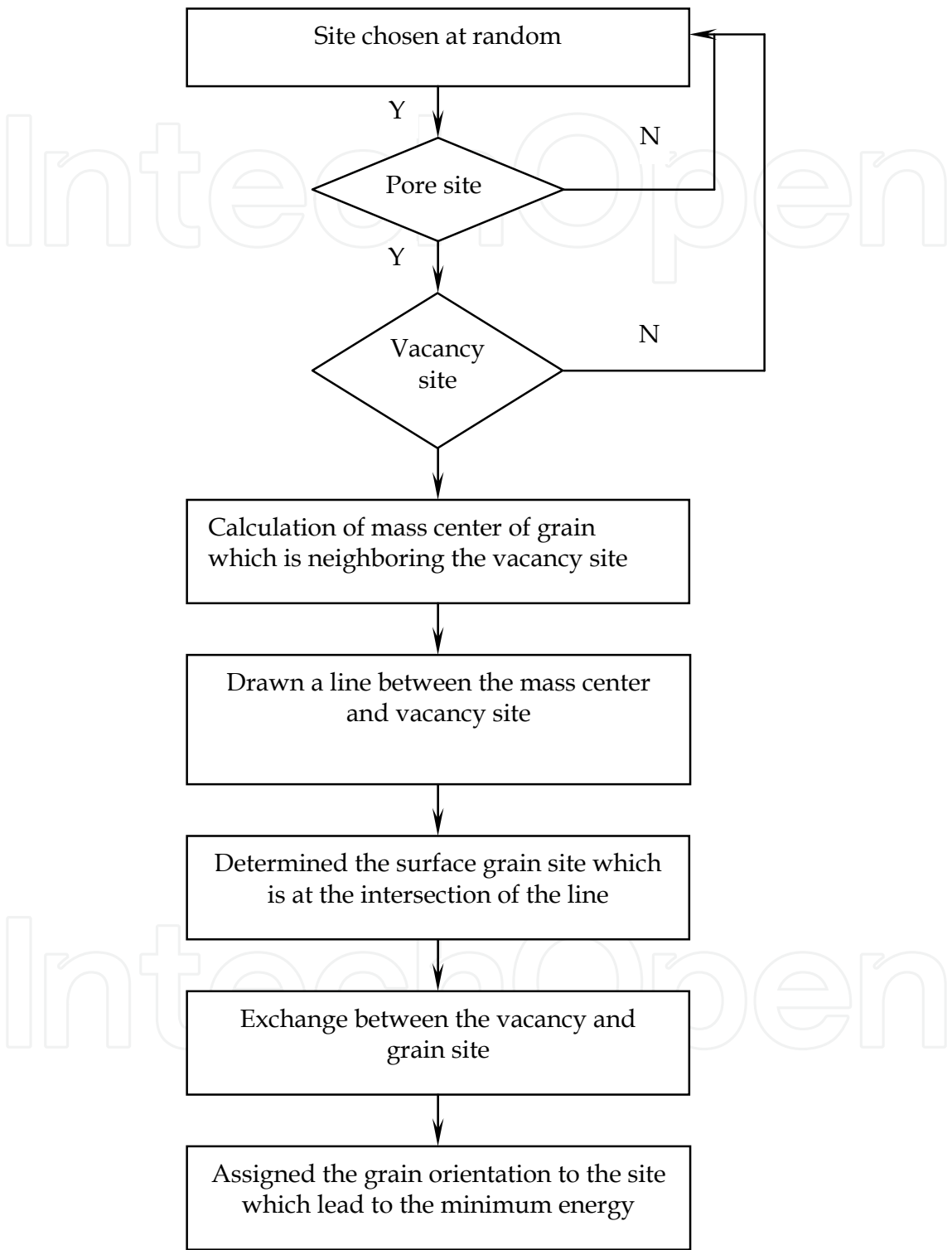
```
┌─────────────────────────────────┐
│        Site chosen at random     │◄──┐
└─────────────────────────────────┘   │
              Y │                      │
                ▼                      │
            ◇ Pore site ◇ ─────N──────┤
                │                      │
              Y │                      │
                ▼                      │
         ◇ Vacancy site ◇ ────N───────┘
                │
                ▼
┌─────────────────────────────────┐
│  Calculation of mass center of   │
│  grain which is neighboring the  │
│         vacancy site             │
└─────────────────────────────────┘
                │
                ▼
┌─────────────────────────────────┐
│  Drawn a line between the mass   │
│    center and vacancy site       │
└─────────────────────────────────┘
                │
                ▼
┌─────────────────────────────────┐
│ Determined the surface grain     │
│ site which is at the             │
│ intersection of the line         │
└─────────────────────────────────┘
                │
                ▼
┌─────────────────────────────────┐
│  Exchange between the vacancy    │
│         and grain site           │
└─────────────────────────────────┘
                │
                ▼
┌─────────────────────────────────┐
│ Assigned the grain orientation   │
│ to the site which lead to the    │
│      minimum energy              │
└─────────────────────────────────┘
```

Fig. 2. Simulation Algorithm of Vacancy Annihilation

During pore annihilation, if the site chosen randomly is a site of vacancy, the grain site for the exchange is chosen at the intersection of a line which is drawn from the site of vacancy

through the mass center of the adjacent grain and the outside boundary of the sintering compact. The grain site is assigned the state of the adjacent grain if the exchange is successful. The pore site, which jumps from inside to outside and coalesces with the others, can visualize the pore exhalation. The grain site which jumps from the outside to the inside can visualize the mass center of the grain migrated to the site of the vacancy. The whole process can conceptualize the densification of ceramic tool materials during fabrication. The site number and the contents of the solid phases are constant to keep the mass conserve during the simulation.

3.4 Simulation conditions

The software is developed with the Visual C++ compiler. The program was implemented in a Pentium-Pro 233MHz computer with 1 GB of RAM. The simulation domain is consisted of 500×500 hexagon sites. The edge length of hexagonal site is 0.6mm in simulation domain, so the area of each site is 0.9353mm^2.

The maximum value of orientation (Q) is 180. It is proved that the simulation results of different Q are nearly indistinguishable from each other when Q>50 is used (Hassold et al, 1990). The simulation time is expressed in term of the number of Monte Carlo Steps (MCS). Because the present simulations are performed on 500×500 sites, one MCS is equal to 250000 attempts in the computational domain. The ratio of the specific grain boundary energy is $J_1:J_2=1:1.4$ in the simulation of microstructural evolution of single-phase ceramic tool material. The ratio of the specific grain boundary energy is $J_{11}:J_{22}:J_{12}:J_{13}:J_{23}=1:4:1:1.4:4.5$ in the simulation of microstructural evolution of two-phase ceramic tool material. These values are comparable to the values of Al_2O_3 and SiC (Handwerker et al, 1990; Tanaka & Kohyama, 2003; Jiao et al, 1997). The simulation numerical data are the average results of the 10 independent simulations so as to eliminate the statistical fluctuations.

(a) Pore Annihilation   (b) Local Magnification near Pore Annihilation
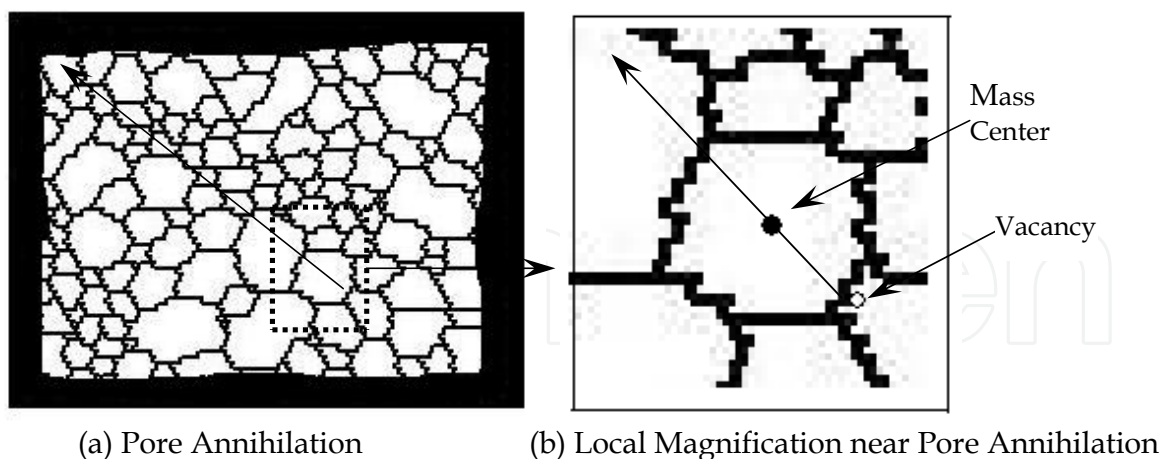
Fig. 3. Schematic of Pore Annihilation

4. Simulation results and discussion

4.1 Simulation of microstructural evolution of single-phase ceramic tool material

As mentioned above, there are 500×500 hexagon sites in the simulation domain, including the 75000 pore sites. That is to say, it is assumed that the porosity of green compact is 30%.

Initialization is needed to perfectly simulate the green compact. The initialization of pore is performed when the mean diameter is 0.29um. The initialized simulation microstructure is shown in Fig. 4. The white region denotes grains, and the black region denotes pores. Fig. 4 (a) is the part of the outside boundary, and the Fig. 4 (b) is the part of the inner. It is found from Fig. 4 (a) that pores exist in the inner of simulation domain and the density is lowest. Neighbor pore sites coalesce together. The bigger the pore is, the more the grain is around the pore. The state of the distribution of simulation microstructure is similar with the real green compact.

(a)   (b)
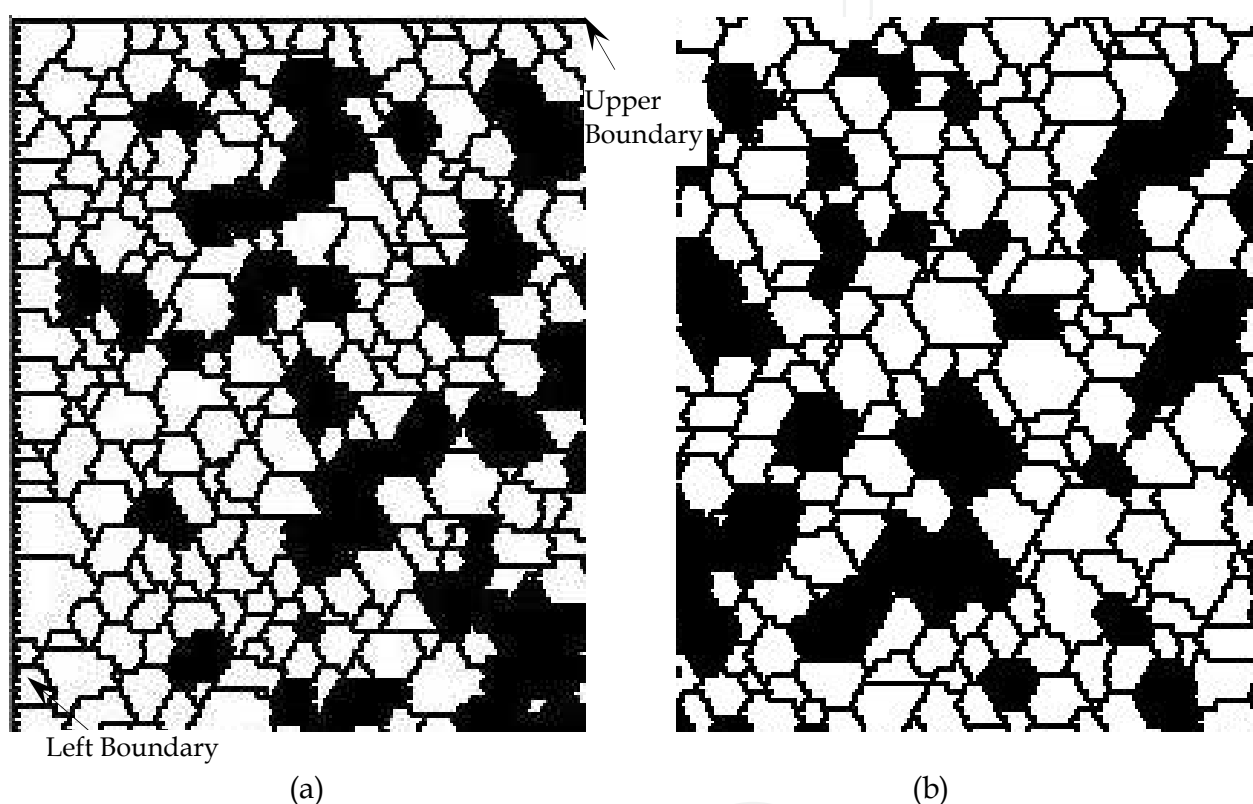
(White region denotes the grain, black region denotes pore)

Fig. 4. Initialized Simulation Microstructure of Single-phase

The resulting microstructure at 100 MCS is shown in Fig. 5. Compared Fig.5 with Fig.4, most of pore sites migrate from the inside to the outside. This is implied that the vacancy is annihilated and exhaled from the inside of simulation domain. Companied by the process, the densification and the grain size also increases. Kingery and Francois (Kingery & Francois, 1965) proposed that pores should exist at the grain boundary, especially, at the triple junction point of grain boundary when the porosity of green compact is fabricated. As shown in Fig.5, the simulation results accord with the theory. It is also seen in Fig.5 that the isolated pore site exists at the grain boundary, which means that the pores diffuse along the grain boundary. It is useful for the pore exhalation and the densification of material.

Left Boundary (a)   (b)
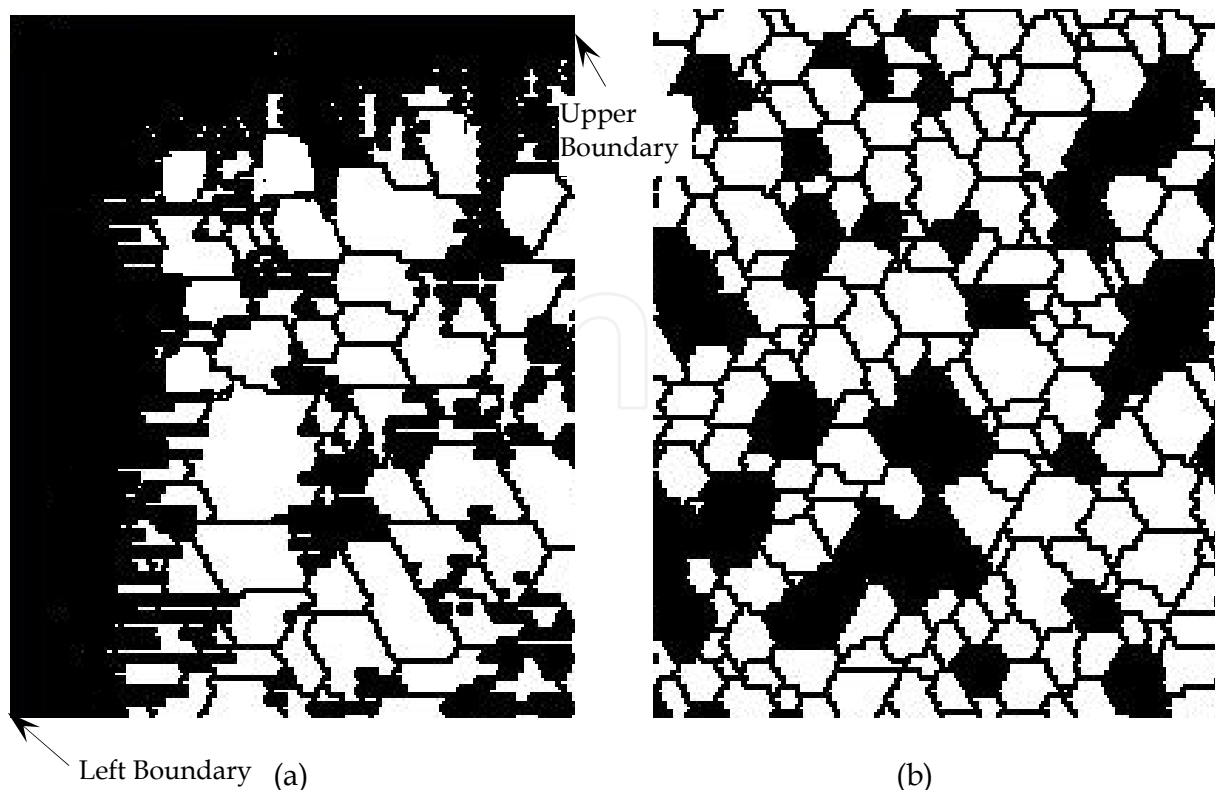
(White region denotes the grain, black region denotes pore)

Fig. 5. Microstructural Evolution of Single-phase Ceramic Tool Materials

4.2 Simulation of microstructural evolution of two-phase ceramic tool material

As mentioned above, there are 500×500 sites in the simulation domain, including 75000 pore sites. It is assumed that the porosity is 30% in the initialization. The second-phase content is 5vol%. In order to perfectly simulate the real green compact, it is necessary to initialize the simulation domain. The initialized simulation microstructure of two-phase ceramic tool materials is shown in Fig.6. Fig.6 (a) is the part of simulation domain at the boundary, and Fig.6 (b) is the part of simulation domain at the inside. It is seen from Fig.6 (a) that the pore sites is in the inside of simulation domain. However, the second-phase sites are the boundary or in the inside of simulation domain. It is similar to the initialized single-phase microstructure where neighbor pore sites coalesce together. The second phase is randomly distributed in the composite and some of them agglomerate. Pore is surrounded by the composite and second-phase particle. It is accordance with the distribution of particle and pore in the green compact.

The simulated microstructure after 100 MCS is shown in Fig.7, where white region denotes the composite, black region denotes the pore and grey region denotes the second-phase particle. Fig.7 (a) is the boundary part of simulation domain. Fig.7 (b) is the inside part of simulation domain. Compared Fig.7 (a) with Fig.6 (a), it is seen that many pore sites jump from the inside of simulation domain to the outside and coalesce with the boundary pores. This implies the isolated pore is annihilated and exhaled from the inside. The density of simulation domain increases with the decrement of pores. It is similar to the simulation results of the single-phase microstructure. Grain size of simulation domain gradually grows. However, by comparison with Fig.5, it is seen from Fig.7 that the rate of grain growth is
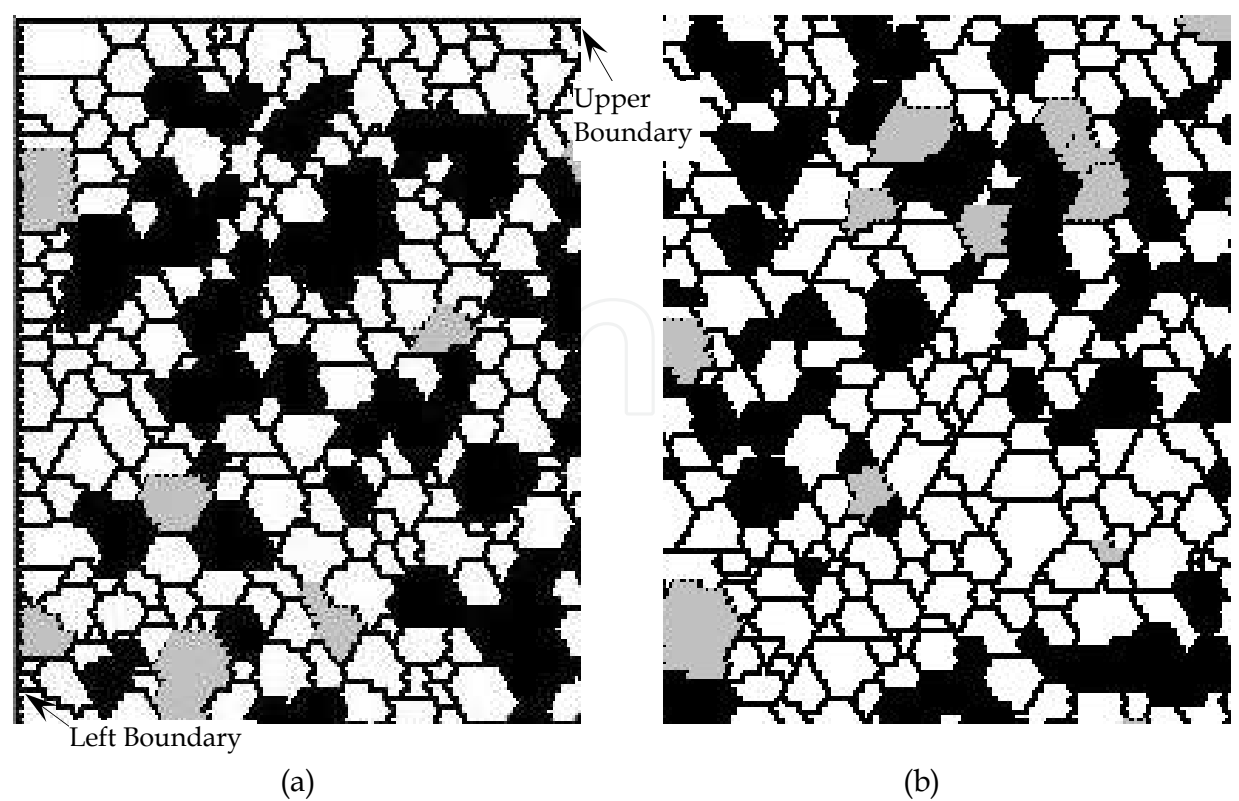
(White region denotes composite phase, black region denotes pore and grey region denotes second phase)

Fig. 6. Two-phase Microstructure of Initialized Simulation Domain
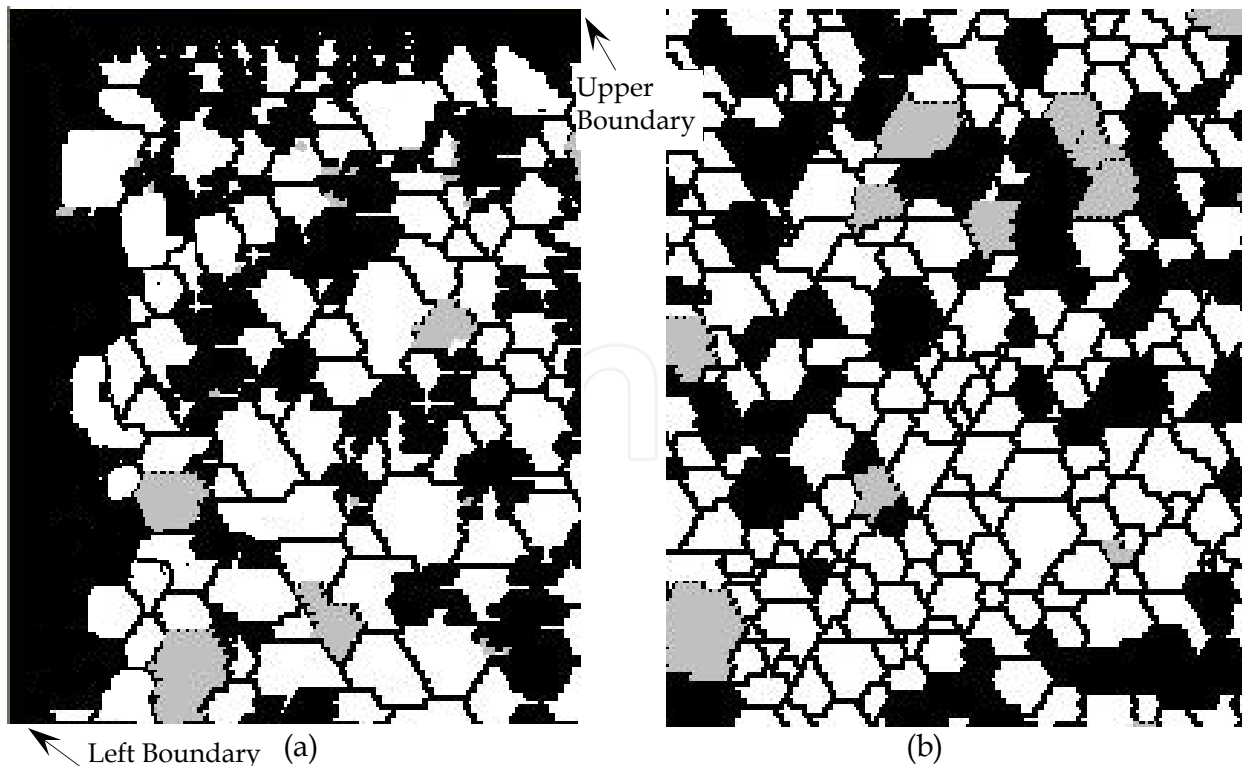
(White region denotes composite phase, black region denotes pore and grey region denotes second phase)

Fig. 7. Two-phase Microstructure of Simulation Domain

slower than that of single-phase grain because the pores continuously migrate and some second-phase particles play a role in pinning effect. The inhibition of pore for composite grain growth is weaker than that of second-phase inhibition for composite grain growth, so that the size of grain around pore is commonly bigger than that of grain around second-phase particle. Just like the simulation results of single-phase system, the pore diffusion along the grain boundary is also found in Fig.7.

The pores in the simulated microstructure gradually disperse and become smaller, and the mass center migrates towards the pores because of pore diffusion along the grain boundary and pore annihilation in both single-phase and two-phase simulation results. And most pores exist at the triple junction point of grain boundary.

4.3 Densification and grain growth

4.3.1 Densification

The simulated microstructure and SEM fracture surface of Al_2O_3 ceramic tool materials are shown in Fig.8. It can be seen from Fig.8 (a) and (b) that some vacancy are surrounded by grains and become voids (or air cavities). As shown in Fig.8 (c), some voids is also found in the Al_2O_3 ceramic tool materials. Voids not only lead to the lower densification, but also lead to the lower mechanical properties because of stress concentration. Some pores are separated from the grain boundary in Fig.8 (a) and (b). The vacancies at the grain boundary, which separate from the grain boundary and become the part of grain, form voids in the process of simulation or sintering, companied by grain growth.

Comparing Fig.8 (a) and (b), it is seen that there are more pores separated from grain boundary in Fig.8 (a) because the grains of single-phase material grow faster than that of two-phase material. Therefore, the perfect content of second phase is useful for the grain refinement as well as elimination or decrement of vacancies, which leads to the improvement of mechanical properties.

The densification of microstructure is calculated by Eq.(15) at simulation time t.

$$\rho = \frac{A_t}{A_0} = \frac{N_g}{N_g + N_p(t)} \tag{15}$$

where, ρ is the densification, A_t is the area of the simulation region at simulation time t, A_0 is the area of the simulation region at the beginning, N_g is solid-phase site number, $N_p(t)$ is the pore-phase site number which is not annihilated at simulation time t.

The relationship between the densification and the simulation time (MCS) is shown in Fig.9. The change trends of the densification curve for single-phase and two-phase material are similar. At some stage of simulation, the densification of two-phase material is slightly lower than that of single-phase material. This is the reason that the growth rate of two-phase grain is slower than that of single-phase grain. At the beginning of simulation, the rate of densification is slower because most pores don't migrate along the grain boundary to form vacancy. The densification is up to 90%, and the ration of pores drastically decreases. Then the rate of densification is gradually slow.

Fig. 10 is the calculated densification curves at final stage sintering of an alumina powder compact (Kang & Jung, 2004) . Comparing Fig.9 and Fig.10, it is found that the densification curves of simulation are very similar to those of calculated results. This means that the simulation result is correct and accurate.
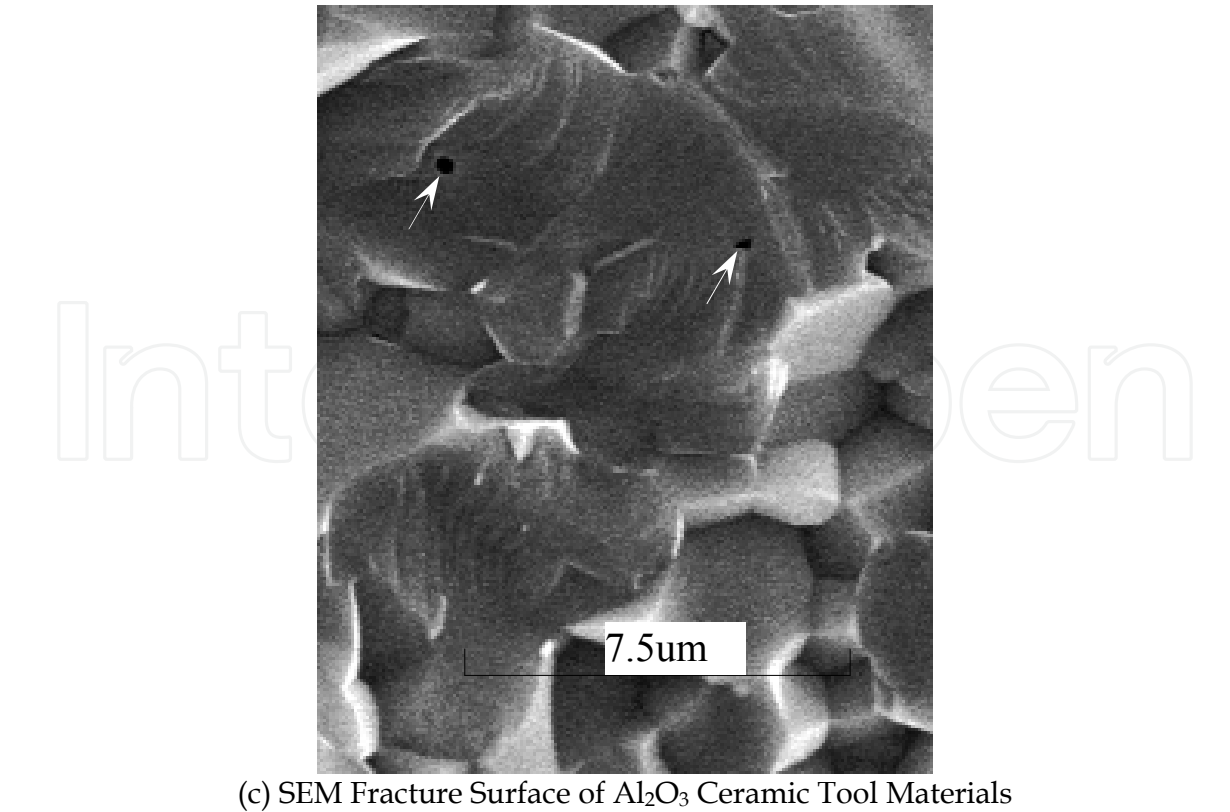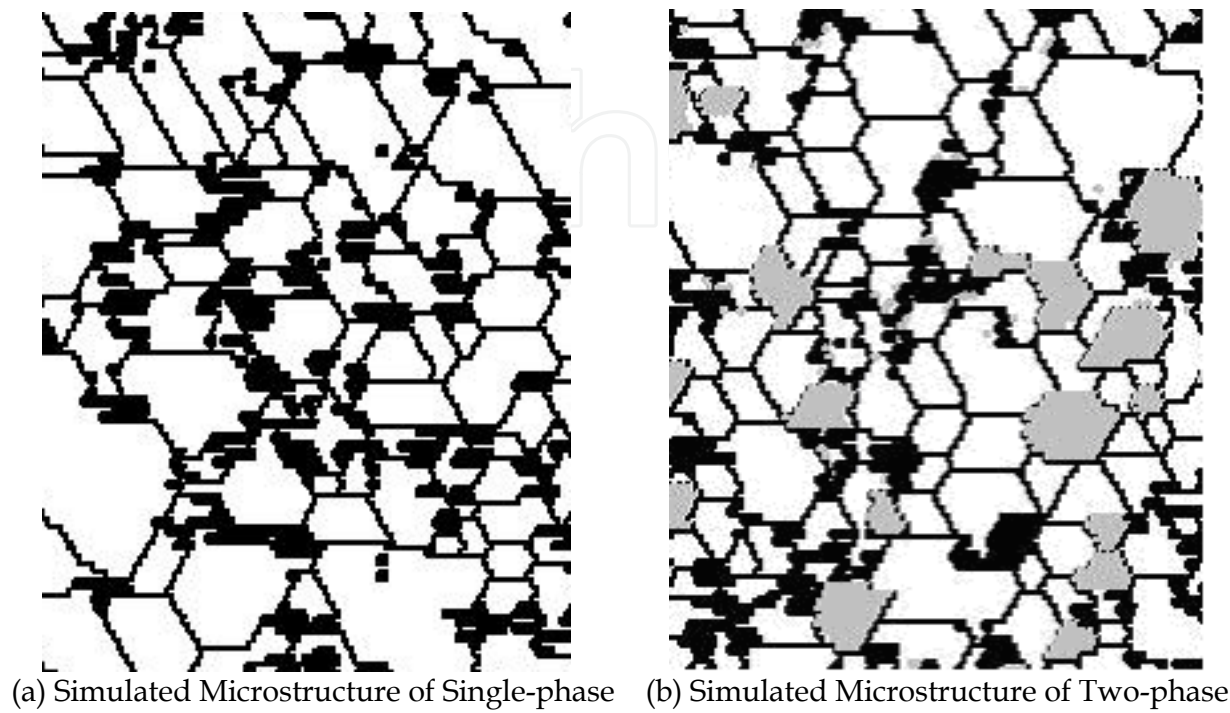

(a) Simulated Microstructure of Single-phase   (b) Simulated Microstructure of Two-phase

7.5um

(c) SEM Fracture Surface of Al$_2$O$_3$ Ceramic Tool Materials

Fig. 8. Simulation Microstructure at 300MCS and Fracture Surface of Al$_2$O$_3$
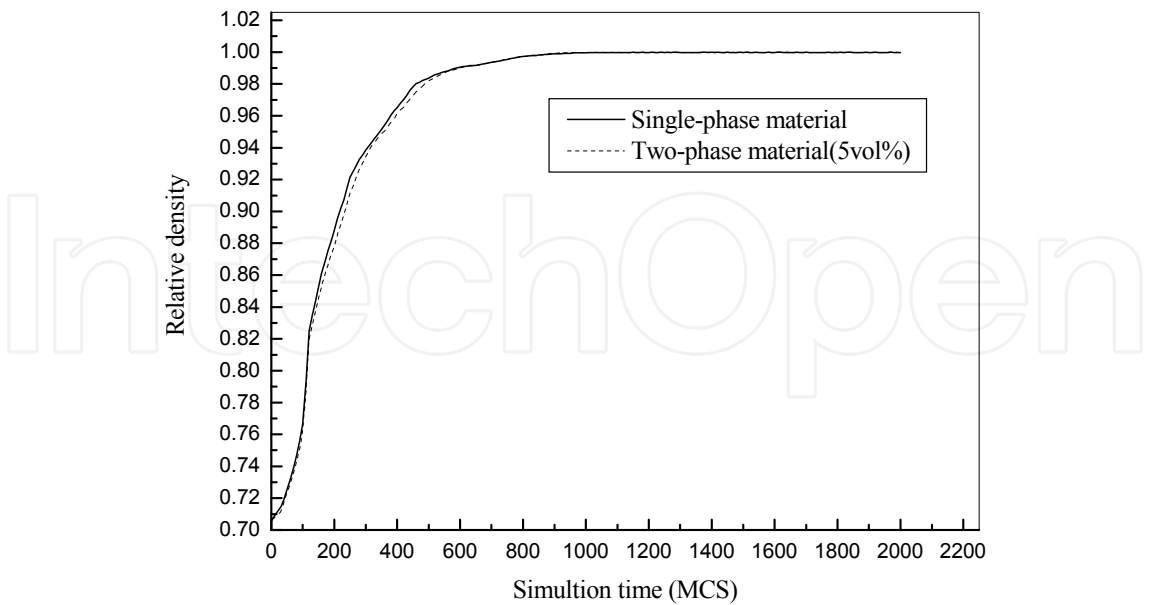
Fig. 9. Relative Density vs. Simulation Time
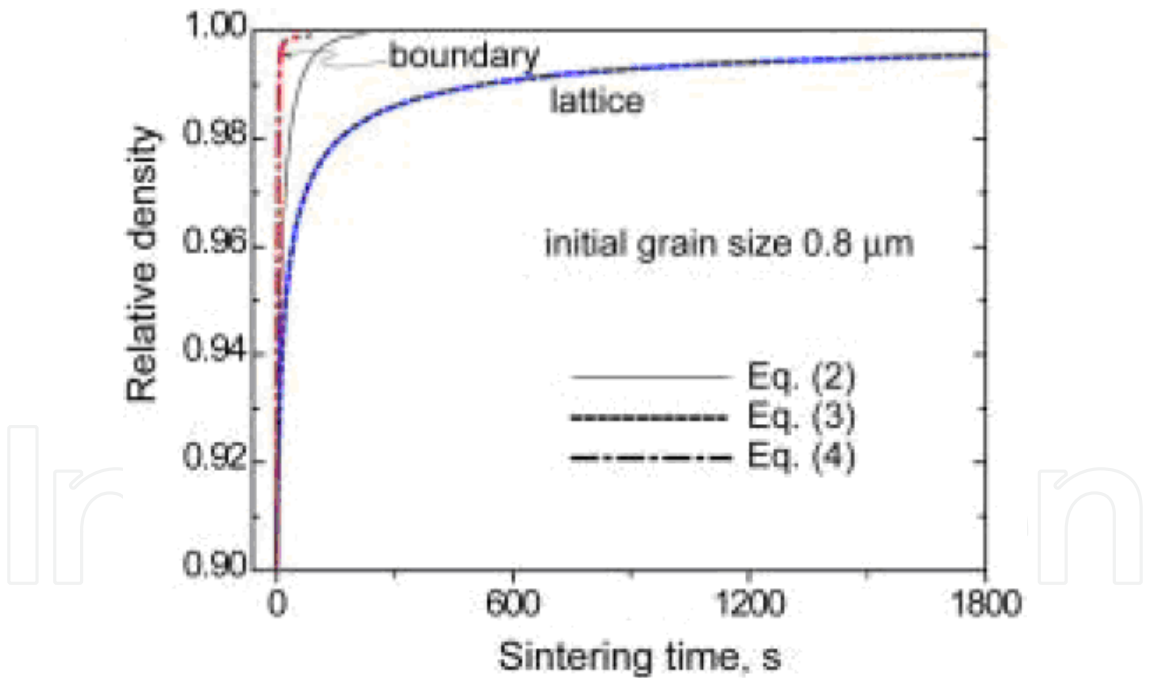
Fig. 10. Calculated Relative Density vs. Sintering Time of an Alumina Powder Compact (Kang & Jung, 2004)

4.3.2 Grain growth

Fig.11 is the relationship between average grain size $\bar{R}$ and simulation time t (MCS). The average grain size of single- and two-phase material grows slowly from 0 to 400 MCS. The average grain size of single-and two-phase material grows fast when the simulation time is

more than 400 MCS. However, the average grain size of single-phase material is bigger than that of two-phase material during the whole process of simulation. The reason can be found from Fig. 9. The densification is lower, that is to say, the content of pore is more, when the simulation time is less 400 MCS. The strong pinned effect of pores on the grain growth leads to a low rate of grain growth. However, the pinned effect of pores on the grain growth which is gradually weak with a decrement of pores leads to a high rate of grain growth, especially after 400 MCS. The rate of grain growth is slow in the whole process because the grain growth is inhibited by not only pores but also second-phase particles and the inhibition of second-phase particles become stronger with the grain growth of composite.
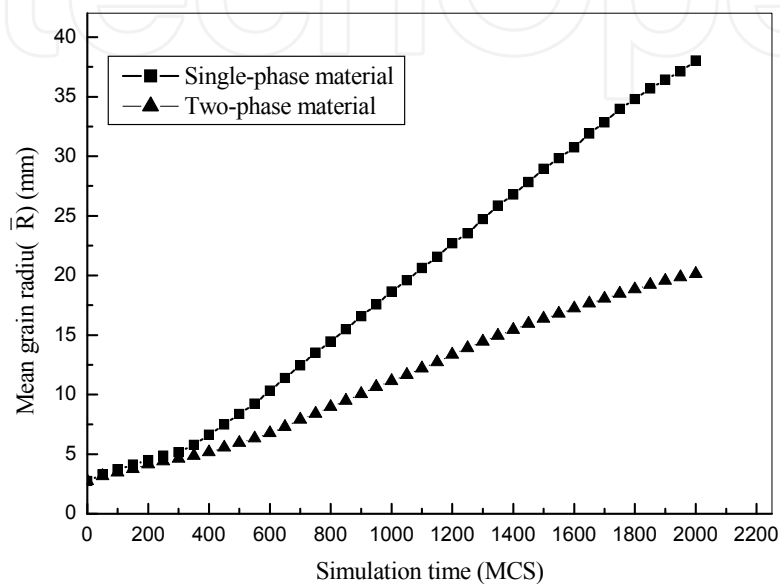
Fig. 11. Average Grain Size ($\bar{R}$) vs. Simulation Time (MCS)

The simulation results have been validated by the hot-press fabrication of Al_2O_3 ceramic tool materials. The fracture surface of the pure Al_2O_3 material and the Al_2O_3/SiC composite material is shown in Fig. 12 (a) and (b), which are fabricated by the hot-press at the same

     (a) Al_2O_3 (b) Al_2O_3/5%SiC
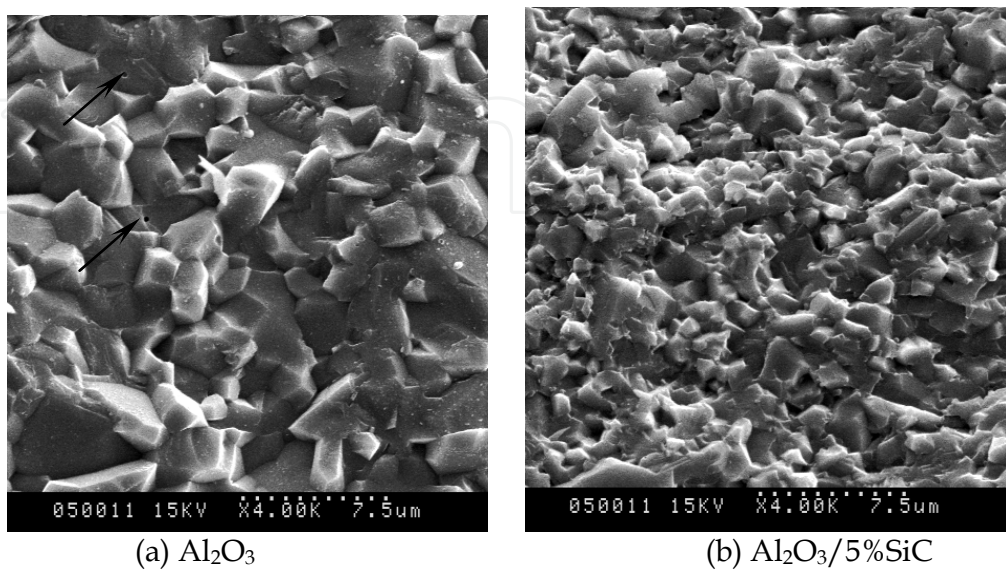
Fig. 12. SEM Fracture Surface of Al_2O_3 Ceramic Tool Materials

fabrication technologies. By the comparison of Fig. 12 (a) and (b), it can be found that the grain size of Fig. 12 (b) is significantly smaller than that of Fig. 12 (a) because the growth of matrix, Al_2O_3, are inhibited by the second phase, SiC. As the arrows are shown in Fig.12 (a), there are voids inside the grains because the grains grow fast and vacancy is separated from the grain boundary, which leads to vacancy trapped by the grain.

According to the theory of sintering, at the final sintering stage the grains grow fast. It is considered that the simulation of microstructure evolution is the final sintering stage of ceramic tool material because the rate of grain growth becomes high and the content of pores drastically decrease after 400MCS.

5. Conclusions

A computer simulation for the sintering processes of single- and two-phase ceramics has been performed using a two-dimensional hexagon lattice model mapped from the realistic microstructure. Different types of boundary energy, the initial grain size, the composition content, the initial pore size and the content of pore are considered in the new simulation model. Because of the different boundary energy, the phase-two and the pore can pin the composite of phase-one and decrease the growth rate of phase-one during the microstructural evolution, which has been invalidated experimentally. The second-phase particle is useful for the refinement of composite grain, which can significantly improve the mechanical properties of ceramic tool material, especially the flexural strength and fracture toughness. The high rate of grain growth is disadvantage of the exhalation of pores according to the result of simulation and experiment. A preliminary investigation shows that the simulation results can accurately prove the relevant sintering kinetics theories and is consistent with the experiment results.

6. Acknowledgement

7. References

Anderson, M. P.; Srolovitz, D. J.; Grest, G.S. (1984). Computer simulation of grain growth-I Kinetcs. Acta Metall., Vol. 32, No. 5, pp. 783-791

Belmonte, M.; Nieto, M. I.; Osendi, M. I.; Miranzo, P. (2006). Influence of the SiC grain size on the wear behavior of Al_2O_3/SiC composites. J. of the European Ceramic Society, Vol. 26, pp. 1273-1279

Bordère, S. (2002). Original Monte Carlo methodology devoted to the study of sintering processes. J. Am. Ceram. Soc., Vol. 85, No. 7, pp. 1845-1852

Braginsky, M.; Tikare, V.; Olevsky, E. (2005). Numerical simulation of solid state sintering. International Journal of Solids and Structures, Vol. 42, pp. 621–636

Chen, I.W.; Hassold, G. N.; Srolovitz, D. J. (1990). Computer simulation of final-stage sintering: II, influence of initial pore size. J. Am. Ceram. Soc., Vol. 73, No. 10, pp. 2865-2872

DeHoff, R. T. (1989). Stereological Theory of Sintering. In: Uskokovic, D.P. et al. (Eds.), Science of Sintering. Plenum Press, New York, pp. 55-71

German, R. M.; Olevsky, E. A. (1998). Modeling grain growth dependence on the liquid content in liquid-phase-sintered materials. Metall. and Mater. Trans., Vol. 29A, No. 12, pp. 3057-3067

Guo, J. K. (1998). The exploration on new approach of strengthening and toughening of ceramic materials. Journal of Inorganic Materials, Vol. 13, No. 1, pp. 23-26

Guo Shiju, (1998). The theory of powder sintering. Metall. Industry Press, Beijing. pp. 30-40

Handwerker, C. A.; Dynys, J. M.; Cannon, R. M. and Coble, R. L. (1990). Dihedral angles in magnesia and alumina: Distributions from surface thermal grooves. J. Am. Ceram. Soc., Vol. 73, No. 5, pp. 1371-1377

Hassold, G. N.; Chen, I-Wei; Srolovtz, D. J. (1990). Computer Simulation of Final-stage: I, Model, Kinetics, and Microstructure. J. Am. Ceram. Soc, Vol. 73, No. 10, pp. 2857-2864

Jagota, A.; Dawson, P. R. (1990). Simulation of the viscous sintering of two particles. J. Am. Ceram. Soc., Vol. 73, No.1, pp. 173-177

Jiao, S.; Jenkins,M. L.; Davidge, R. W. (1997). Interfacial Fracture Energy-mechanical Behaviour Relationship in Al_2O_3/SiC and Al_2O_3/TiN Nanocomposites. Acta mater., Vol. 45, No. 1, pp. 149-156

Jin, Z. H.; Gao, J. Q.; Qiao G. J. (2002). Ceramic Material for Engineering[M], Xi'an: Xi'an Jiaotong University Press, P. R. China.

Kang, S. L.; Jung, Y. (2004). Sintering kinetics at final stage sintering: model calculation and map construction. Acta Mater., Vol. 52, No. 15, pp. 4573-4578

Kingery, W. D; Francois, B. (1965). Grain Growth in Porous Compacts. J Am Ceram Soc., Vol. 48, pp. 546-547

Lang, F. F. (1982). Transformation toughening part 1 size effects associated with the thermodynamics of the constrained transformation. J. Mater Sci., Vol. 17, pp. 225-234

Myers, N.; Meuller, Tim; German, R. (1989). Production of Porous Refractory Metals with Controlled Pore Size. In Particle Packing Characteristics, Metal Powder Industries Federation, Edited by Randall German, pp. 298-300

Srolovitz, D. J.; Anderson, M. P. Sahni P. S. (1984). Computer simulation of grain growth-II Grain Size Distribution, Topology, and Local Dynamics. Acta Metall., Vol. 32, No. 5, pp. 793-802

Mori, K. (2006). Finite element simulation of powder forming and sintering. Comput. Methods Appl. Mech. Engrg., Vol. 195, pp. 6737-6749

Mukhopadhyay, A.; Basu, B.; Das Bakshi, S. (2007). Pressureless sintering of ZrO_2-ZrB_2 composites: Microstructure and properties. International Journal of Refractory Metals & Hard Materials, Vol. 25, pp. 179-188

Tanaka, K.; Kohyama, M. (2003). Atomic Structure Analysis of Σ=3, 9 and 27 Boundary, and Multiple Junctions in β-SiC. JEOL, Vol. 28, No. 2, pp. 8-10

Tikare, V.; Braginsky, M,;, Olevsky, E. A. (2003). Numerical simulation of solid-state sintering I, sintering of three particles. J. Am. Ceram. Soc., Vol. 86, No. 1, pp. 49-53

Tikare; V., Holm; E. A. (1998). Simulation of grain growth and pore migration in a thermal gradient. J. Am. Ceram. Soc., Vol. 81, No 3, pp. 480-484

Wakai, F.; Shinoda,Y.; Akastu,T. (2004). Methods to calculate sintering stress of porous materials in equilibrium. Acta Materialia, Vol. 52, pp. 5621-5631

Wakai, F; Yoshida, M.; Shinoda, Y.; Akastu, T. (2005). Coarsening and grain growth in singering of two particles of different sizes. Acta Mater. Vol. 53, pp. 1361-1371
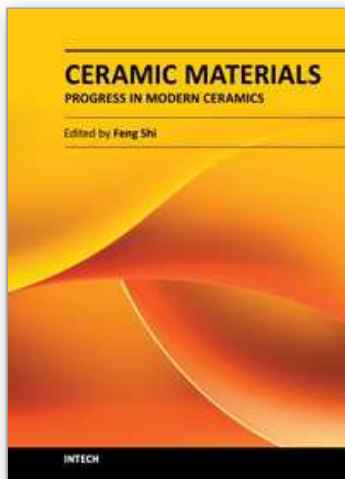
Ceramic Materials - Progress in Modern Ceramics

Edited by Prof. Feng Shi

This text covers ceramic materials from the fundamentals to industrial applications. This includes their impact on the modern technologies, including nano-ceramic, ceramic matrix composites, nanostructured ceramic membranes, porous ceramics, and the sintering theory model of modern ceramics.

How to reference

In order to correctly reference this scholarly work, feel free to copy and paste the following:

INTECH
open science | open minds